

Crystalline electric fields and the ground state of $\text{Ce}_3\text{Rh}_4\text{Pb}_{13}$ D. A. Sokolov,^{1,*} M. C. Aronson,¹ C. Henderson,² and J. W. Kampf³¹Department of Physics, University of Michigan, 450 Church Street, Ann Arbor, Michigan 48109-1040, USA²Department of Geological Sciences, University of Michigan, 1100 North University, Ann Arbor, Michigan 48109-1005, USA³Department of Chemistry, University of Michigan, 930 North University, Ann Arbor, Michigan 48109-1055, USA

(Received 30 November 2006; published 9 August 2007)

We have succeeded in synthesizing single crystals of an intermetallic compound $\text{Ce}_3\text{Rh}_4\text{Pb}_{13}$. Magnetic susceptibility measurements indicate that the Ce moments are highly localized despite the metallic character of the electrical resistivity. Heat capacity measurements reveal that the crystalline electric field lifts the sixfold degeneracy of the Ce^{3+} ground state, with the excited quartet separated by approximately 60 K from the doublet ground state. The magnetic field dependence of the heat capacity at low temperature indicates a further splitting of the doublet, but no sign of magnetic order was found above 0.35 K.

DOI: 10.1103/PhysRevB.76.075109

PACS number(s): 71.20.Eh, 75.40.Cx

I. INTRODUCTION

Rare-earth-based intermetallic compounds continue to attract a great deal of interest due to the richness of the magnetic and electronic phenomena observed in these systems.^{1,2} In particular, non-Fermi-liquid behavior was found in the vicinity of zero temperature magnetic phase transitions, often manifested by power-law temperature dependence of the magnetic susceptibility and logarithmic temperature dependence of the heat capacity divided by the temperature. Synthesis of novel rare-earth intermetallics in a pure form, typically achieved by growing single crystals, is instrumental in identifying new physics associated with the magnetic ordering at zero temperature.

The compounds with a general formula $R_3\text{Rh}_4\text{Sn}_{13}$, where R is a rare-earth element, were first synthesized by Remeika *et al.*³ It was found that the materials with $R=\text{Tm}$, Lu , and Y are superconductors, while compounds with $R=\text{Tb}$, Dy , and Ho order magnetically. The $R=\text{Eu}$ member of this family demonstrated reentrant superconductivity, in turn destroyed by the onset of ferromagnetic order. Subsequently, other members of a broader family $R_3T_4X_{13}$, where T = transitional metal and X is metalloid from Group IV or V, were studied and found to order antiferromagnetically at low temperatures.⁴⁻⁶ Interestingly, heavy fermion $\text{Ce}_3\text{Ir}_4\text{Sn}_{13}$, which crystallizes into a primitive cubic structure (space group $Pm\bar{3}n$), orders antiferromagnetically and demonstrates an intriguing double peak feature on the temperature dependence of the heat capacity near the ordering temperature.^{4,7} In cubic (space group $Pm\bar{3}n$) heavy fermion $\text{Ce}_3\text{Pt}_4\text{In}_{13}$, the Kondo and Ruderman-Kittel-Kasuya-Yosida energy scales are nearly equivalent and their balance can be changed by applied pressure.⁸ Recently, new cubic $\text{Ln}_3\text{Co}_4\text{Sn}_{13}$ compounds with $\text{Ln}=\text{Ce}$ and La (space group $Pm\bar{3}n$) were reported.^{9,10} $\text{Ce}_3\text{Co}_4\text{Sn}_{13}$ is a heavy fermion, which does not order magnetically above $T\sim 0.35$ K, while its La counterpart is a conventional superconductor.

Such a panorama of magnetic properties and the variety of electronic ground states in cubic $R_3T_4X_{13}$ motivated us to synthesize a compound with $T=\text{Rh}$ and $X=\text{Pb}$. We report here a systematic study of the physical properties of a cubic metallic compound $\text{Ce}_3\text{Rh}_4\text{Pb}_{13}$, which we carried out in

search for other materials lying close to the quantum critical point.

II. EXPERIMENTAL DETAILS

Single crystals of $\text{Ce}_3\text{Rh}_4\text{Pb}_{13}$ were grown from Pb flux. Single crystal x-ray diffraction experiments were carried out at room temperature using a Bruker 1K charge coupled device based single crystal diffractometer with $\text{Mo } K\alpha$ radiation. The structure was solved and refined using SHELXTL package.¹¹ Electron microprobe measurements were made at a 20 kV accelerating voltage on a CAMECA SX100 electron microprobe analyzer using $\text{Ce } L\alpha$, $\text{Rh } L\alpha$, and $\text{Pb } M\alpha$ x-ray lines calibrated with synthetic CePO_4 , synthetic CeRhSn , and natural PbS standards. The magnetic susceptibility was measured using a Quantum Design Magnetic Phenomena Measurement System at temperatures from 1.8 to 300 K. The electrical resistivity ρ of $\text{Ce}_3\text{Rh}_4\text{Pb}_{13}$ was measured by the conventional four-probe method between 0.35 and 300 K in zero magnetic field. Measurements of the heat capacity were performed using a Quantum Design Physical Property Measurement System at temperatures from 0.35 to 70 K and in magnetic fields up to 2 T.

III. RESULTS AND DISCUSSION

Electron microprobe experiments found the composition of the crystals slightly off-stoichiometric, with the elemental ratios for $\text{Ce}:\text{Rh}:\text{Pb}$ of $2.89\pm 0.05:4.40\pm 0.10:12.71\pm 0.07$ uniform over the surface of the crystals. Single crystal x-ray diffraction experiments confirmed this stoichiometry and found a cubic structure (space group $Pm\bar{3}n$, No. 223) with $a=10.0010(6)$ Å, which is shown in Fig. 1. The unit cell contains 2 f.u. Corrections were made for absorption and extinction, and the atomic positions were refined with anisotropic displacement parameters. The results of the x-ray diffraction experiments are summarized in Tables I and II.

The temperature dependence of the electrical resistivity ρ is that of a good metal (Fig. 2). ρ decreases from the value of $100 \mu\Omega \text{ cm}$ at 300 K to $\sim 30 \mu\Omega \text{ cm}$ at 2 K. The inset of Fig. 2 shows a partial superconducting transition at $T_c=2$ K, which we believe is due to trace amounts of superconducting

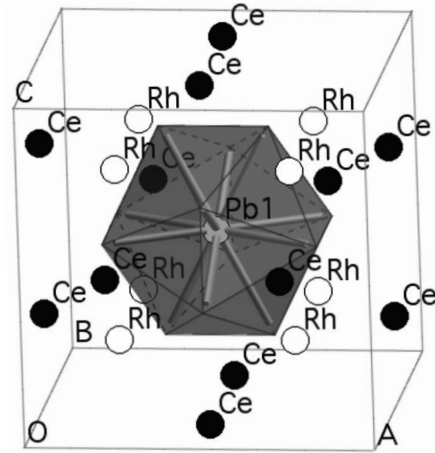


FIG. 1. Crystal structure of $\text{Ce}_3\text{Rh}_4\text{Pb}_{13}$. Single unit cell is shown highlighting the Pb1(Pb2)_{12} icosahedron (light gray).

RhPb_2 .¹² Measurements of the Meissner effect confirmed these conclusions, finding a volume fraction of less than 1% for the proposed RhPb_2 inclusions.

Measurements of the magnetic susceptibility found that the Ce ions in $\text{Ce}_3\text{Rh}_4\text{Pb}_{13}$ are well localized. The temperature dependence of the dc magnetic susceptibility χ and its inverse are shown in Fig. 3. χ increases monotonically with decreasing temperature, and the inverse of χ was fitted to a straight line between 34 and 300 K (Fig. 3). The fit yielded a Weiss temperature $\Theta = -39 \pm 0.7$ K, suggesting that the magnetic correlations in $\text{Ce}_3\text{Rh}_4\text{Pb}_{13}$ are antiferromagnetic, and an effective magnetic moment $\mu_{\text{eff}} = 2.6 \pm 0.1 \mu_B$ per Ce ion, close to the $2.54 \mu_B$ expected for a free Ce^{3+} ion. Below ~ 30 K, $1/\chi$ demonstrates a pronounced downward curvature, as is characteristic of systems with a substantial crystalline electric field (CEF) splitting of the ground state of Ce^{3+} or antiferromagnetic correlations. χ is found to be completely isotropic in the measured temperature range, which is expected for a cubic system such as $\text{Ce}_3\text{Rh}_4\text{Pb}_{13}$, where Ce ions occupy only equivalent sites in the unit cell.

Heat capacity measurements confirm that the Ce moments are only weakly coupled to the conduction electrons. The temperature dependence of the heat capacity $C(T)$ was measured in zero field and at temperatures as high as 70 K [Fig. 4(a)]. We have estimated the phonon contribution to the heat capacity C_{ph} using the Debye expression and a Debye temperature $\theta_D = 163 \pm 10$ K. C_{ph} is subtracted from $C(T)$ in

TABLE II. Selected bond lengths (\AA) in $\text{Ce}_3\text{Rh}_4\text{Pb}_{13}$ at 293 K.

Ce–Pb(1)	5.591(1)	Ce–Pb(2) ($\times 8$)	3.5220(7)
Ce–Pb(2) ($\times 4$)	3.4897(9)	Ce–Rh	3.5359(2)
Rh–Pb(2)	2.7321(4)	Rh–Pb(1)	4.331(1)
Pb(1)–Pb(2)	3.4423(10)	Pb(2)–Pb(2)	3.3182(15)
Pb(1)–Pb(1)	8.661(1)		

Fig. 4(a) to isolate the remaining magnetic and electronic contributions to the heat capacity. The latter is expected to result in a component of the heat capacity which is linear in temperature, $C_{\text{el}} = \gamma T$.

C/T is plotted as a function of T^2 in Fig. 4(b), demonstrating that the electronic contribution is found only over a narrow range of temperatures, yielding $\gamma = 15 \pm 2$ mJ/mole K^2 . We conclude that the purely electronic contribution to the heat capacity is very small, as would be expected for weakly correlated conduction electrons or, alternatively, for a low density of conduction electrons for $\text{Ce}_3\text{Rh}_4\text{Pb}_{13}$. In either case, we conclude that the Kondo temperature for this system is very small.

The crystal electric field scheme for these localized Ce moments was established from heat capacity measurements. The cubooctahedral point symmetry at the Ce site splits the $J=5/2$ Hund's rule multiplet of Ce^{3+} into three doublets. However, if the higher-lying doublets are close in energy, they can be viewed as a quartet. We suggest that the broad maximum found in $C - C_{\text{ph}} = C_{\text{mag}}$ near 23 K in Fig. 4(a) is a Schottky anomaly, which corresponds to a thermally activated transition from a doublet ground state to the higher-lying quartet, separated by an energy gap of 60 K as illustrated in the inset (1) in Fig. 4(a). Therefore, the full Ce^{3+} magnetic moment can only be found above 60 K. Below ~ 60 K, we expect to find a reduced and temperature dependent effective magnetic moment.

Given the high crystal symmetry, the relatively close Ce–Ce spacing, and the absence of a measurable Kondo effect, we searched for evidence that magnetic order occurs in this system. At temperatures below 3 K, the heat capacity demonstrates a monotonic increase, perhaps indicative of incipient order, shown in the inset (2) of Fig. 4(a).

However, the application of a magnetic field shows that this is the high temperature side of another broad peak, which can be a signature of either the Schottky-type transition or the Kondo heat capacity, with the Kondo temperature

TABLE I. Structural parameters of $\text{Ce}_3\text{Rh}_4\text{Pb}_{13}$ at 293 K. Space group is $Pm-3n$, $a = 10.0010(6)$ \AA , $V = 1000.30(10)$ \AA^3 , and calculated density is 11.705 g/cm. Agreement indices: $R_1 = 0.0398$, $wR_2 = 0.1158$; goodness of fit 1.256.

Atom	Site	x	y	z	U_{eq}^a (\AA^2)
Pb(1)	2a	0	0	0	0.027(1)
Pb(2)	24k	0.1557(1)	0.3070(1)	0	0.024(1)
Ce	6d	0	0.5	0.25	0.023(1)
Rh	8e	0.25	0.25	0.25	0.020(1)

^a U_{eq} is defined as one-third of the trace of the orthogonalized U_{ij} tensor.

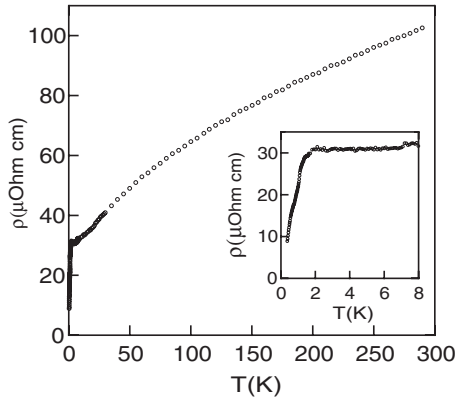


FIG. 2. Temperature dependence of the electrical resistivity of $\text{Ce}_3\text{Rh}_4\text{Pb}_{13}$.

$T_K < 1$ K. When magnetic field is applied, the upturn develops into a broad maximum, which shifts to higher temperatures with increasing field (Fig. 5).

In our calculations of the Kondo heat capacity, we have used a model proposed by Rajan *et al.*¹³ for the Coqblin-Schrieffer impurities. We have plotted the results of our calculations for the single channel $S=1/2$ impurity model (for magnetic field of 2 T) with the varied parameter $T_K = 0.16$ K in Fig. 5. The width of the Kondo heat capacity peak is reasonable, but the magnitude of the Kondo heat capacity is smaller than the measured one at all temperatures. A better fit to the pronounced maximum found in the 2 T data was obtained assuming a Schottky-type transition between levels of equal degeneracies. A magnetic field of 2 T splits the ground state doublet into two singlets separated by an energy gap of 2 K, indicating that the low-lying doublet ground state is itself split, with an extrapolated energy gap of ~ 1 K in zero field. We conclude that even if the f electrons of Ce^{3+} are partially coupled to a conduction band, the corresponding energy scale of 0.16 K is too small compared to the splitting of the ground state doublet. Therefore $\text{Ce}_3\text{Rh}_4\text{Pb}_{13}$ remains a local moment system on energy scales as small as 1 K.

The temperature dependence of the entropy calculated from the heat capacity data of Fig. 4(a) is shown in Fig. 6.

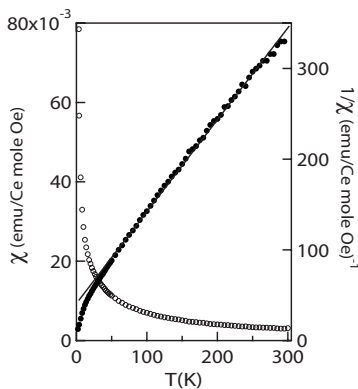


FIG. 3. Temperature dependence of the magnetic susceptibility (○) and its inverse (●) of $\text{Ce}_3\text{Rh}_4\text{Pb}_{13}$ measured in 1000 Oe.

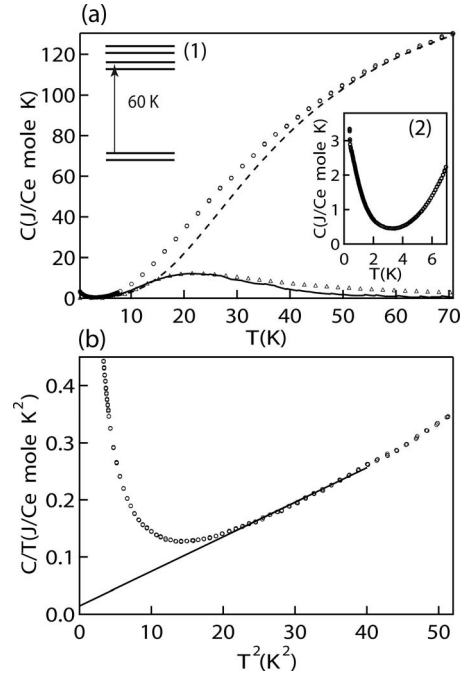


FIG. 4. (a) Temperature dependence of the heat capacity C (○) of $\text{Ce}_3\text{Rh}_4\text{Pb}_{13}$ measured in zero field. The dashed line is the estimated lattice heat capacity. Δ marks the electronic and magnetic parts of the total heat capacity. The solid line is the Schottky fit. Inset (1): Proposed CEF scheme for $\text{Ce}_3\text{Rh}_4\text{Pb}_{13}$. Inset (2): Temperature dependence of the heat capacity C (○) of $\text{Ce}_3\text{Rh}_4\text{Pb}_{13}$ below 7 K. (b) The electronic part of the heat capacity $C_{el} = \gamma T$ is determined from this plot of $C/T = \gamma + \beta T^2$.

The entropy increases sharply up to $T=2$ K and almost saturates at the value of $\sim 0.62R \ln 2$ and increases as the temperature is further increased. The reduced value of the entropy is likely due to the neglected part of the heat capacity below $T=0.35$ K, inaccessible in our measurements.

The temperature dependence of the magnetic susceptibility χ is in good qualitative agreement with the crystal field scheme deduced from the heat capacity measurements in $\text{Ce}_3\text{Rh}_4\text{Pb}_{13}$. Figure 7 shows the temperature dependence of the effective magnetic moment defined as $\mu_{eff}(T) = \sqrt{(3k_B T \chi)}/N$. Well above $T=60$ K, which is the energy

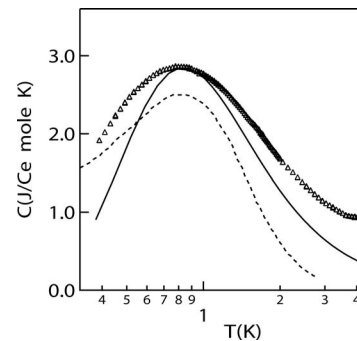


FIG. 5. Temperature dependence of the heat capacity of $\text{Ce}_3\text{Rh}_4\text{Pb}_{13}$ measured in a magnetic field of 2 T (Δ). The solid line is the Schottky fit; the dashed line is the Kondo fit.

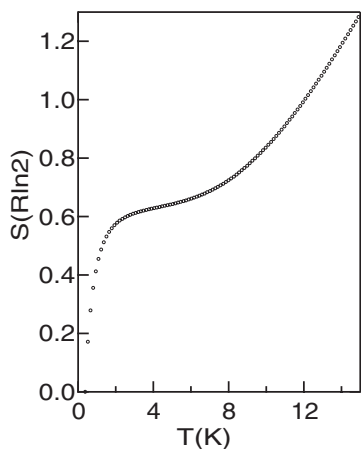


FIG. 6. Temperature dependence of the zero field entropy of $\text{Ce}_3\text{Rh}_4\text{Pb}_{13}$.

splitting between the ground state doublet and the excited quartet split by the CEF, μ_{eff} is close to the value of $2.54\mu_B$ expected for a free Ce^{3+} ion. At lower temperatures, CEF partially lifts the degeneracy of the ground state and reduces the total angular momentum J . This, in turn, lowers the μ_{eff} as $\mu_{eff} \propto \sqrt{J(J+1)}$.

IV. CONCLUSION

Taken together, our data reveal $\text{Ce}_3\text{Rh}_4\text{Pb}_{13}$ to be an almost completely localized moment system, with no indication of magnetic order above 0.35 K or the Kondo effect. We infer that $\text{Ce}_3\text{Rh}_4\text{Pb}_{13}$ most likely lies at the weakly coupled

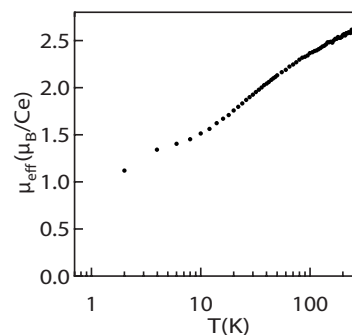


FIG. 7. Temperature dependence of the effective magnetic moment $\mu_{eff}(T) = \sqrt{3k_B T \chi} / N$ of $\text{Ce}_3\text{Rh}_4\text{Pb}_{13}$.

extreme of the Doniach phase diagram.¹⁴ Our data suggest that despite high crystal symmetry and closely spaced Ce moments, $\text{Ce}_3\text{Rh}_4\text{Pb}_{13}$ apparently avoids magnetic order through the successive lifting of the Ce degeneracy and the consequent suppression of the Ce moment. It will be very interesting to extend our measurements to temperatures below 0.35 K to ascertain whether $\text{Ce}_3\text{Rh}_4\text{Pb}_{13}$ orders magnetically.

ACKNOWLEDGMENTS

Work at the University of Michigan was supported by the National Science Foundation under Grant No. NSF-DMR-0405961. The electron microprobe used in this study was partially funded by Grant No. EAR-99-11352 from the National Science Foundation. D.A.S. acknowledges useful conversations with P. Schlottmann.

*sokolov@bnl.gov

¹G. R. Stewart, *Rev. Mod. Phys.* **73**, 797 (2001).

²Y. Ōnuki, R. Settai, K. Sugiyama, T. Takeuchi, T. C. Kobayashi, Y. Haga, and E. Yamamoto, *J. Phys. Soc. Jpn.* **73**, 769 (2004).

³J. P. Remeika, G. P. Espinosa, A. S. Cooper, H. Barz, J. M. Rowell, D. B. McWhan, J. M. Vandenberg, D. E. Moncton, Z. Fisk, L. D. Woolf, H. C. Hamaker, M. B. Maple, G. Shirane, and W. Thomlinson, *Solid State Commun.* **34**, 923 (1980).

⁴S. Takayanagi, H. Sato, T. Fukuhara, and N. Wada, *Physica B* **199-200**, 49 (1994).

⁵Yuji Aoki, Tadashi Fukuhara, Hitoshi Sugawara, and Hideyuki Sato, *J. Phys. Soc. Jpn.* **65**, 1005 (1996).

⁶Chiyoko Nagoshi, Ryunosuke Yamamoto, Keitaro Kuwahara, Hajime Sagayama, Daich Kawana, Masahumi Kongi, Hitoshi Sugawara, Yuji Aoki, Hideyuki Sato, Tetsuya Yokoo, and Masatoshi Arai, *J. Phys. Soc. Jpn.* **75**, 044710 (2006).

⁷C. Nagoshi, H. Sugawara, Y. Aoki, S. Sakai, M. Kohgi, H. Sato, T. Onimaru, and T. Sakakibara, *Physica B* **359-361**, 248 (2005).

⁸M. F. Hundley, J. L. Sarrao, J. D. Thompson, R. Movshovich, M. Jaime, C. Petrovic, and Z. Fisk, *Phys. Rev. B* **65**, 024401 (2001).

⁹Evan Lyle Thomas, Han-Oh Lee, Andrew N. Bankston, Samuel MaQuilon, Peter Klavins, Monica Moldovan, David P. Young, Zachary Fisk, and Julia Chan, *J. Solid State Chem.* **179**, 1642 (2006).

¹⁰A. L. Cornelius, A. D. Christianson, J. L. Lawrence, V. Fritsch, E. D. Bauer, J. L. Sarrao, J. D. Thompson, and P. G. Pagliuso, *Physica B* **378-380**, 113 (2006).

¹¹G. M. Sheldrick, *SHELXTL*, V. 6.12 Bruker Analytical X-ray Madison, WI, 2001.

¹²M. F. Gendron and R. E. Jones, *J. Phys. Chem. Solids* **23**, 405 (1962).

¹³V. T. Rajan, J. H. Lowenstein, and N. Andrei, *Phys. Rev. Lett.* **49**, 497 (1982).

¹⁴S. Doniach, *Physica B & C* **91**, 231 (1977).